

Training cascaded networks for speeded decisions using a temporal-difference loss

Michael L. Iuzzolino^{1,2} Michael C. Mozer^{1,2} Samy Bengio¹

Abstract

Although deep feedforward neural networks share some characteristics with the primate visual system, a key distinction is their dynamics. Deep nets typically operate in *sequential* stages wherein each layer fully completes its computation before processing begins in subsequent layers. In contrast, biological systems have *cascaded* dynamics: information propagates from neurons at all layers in parallel but transmission is gradual over time. In our work, we construct a cascaded ResNet by introducing a propagation delay into each residual block and updating all layers in parallel in a stateful manner. Because information transmitted through skip connections avoids delays, the functional depth of the architecture increases over time and yields a trade off between processing speed and accuracy. We introduce a temporal-difference (TD) training loss that achieves a strictly superior speed-accuracy profile over standard losses. The CASCADINGTD model has intriguing properties, including: typical instances are classified more rapidly than atypical instances; CASCADINGTD is more robust to both persistent and transient noise than is a conventional ResNet; and the time-varying output trace of CASCADINGTD provides a signal that can be used by ‘meta-cognitive’ models for OOD detection and to determine when to terminate processing.

1. Introduction

A synergistic relationship has long existed between theories of human vision and deep neural networks. Deep nets have been used as a model of human vision (Kriegeskorte, 2015; Lindsay, 2020). And deep nets have been fruitfully

¹Google Research, Brain Team ²Department of Computer Science, University of Colorado, Boulder, United States of America. Correspondence to: Michael L. Iuzzolino <michael.iuzzolino@colorado.edu>, Michael C. Mozer <mcmozer@google.com>.

informed by neuroscience. The most compelling such example is of course convolutional networks, which have adopted properties of primate cortical neuroanatomy including a hierarchical layered architecture, local receptive fields, and spatial equivariance (Fukushima, 1980). Despite the synergy, key properties of biological information processing systems have been set aside in the design of neural networks. In this article, we consider four fundamental but neglected properties. First, the brain consists of dedicated hardware and all neurons in all layers update continually and in parallel. Second, information transmission between neurons is relatively slow. Third, unrefined and possibly incomplete neural state in one layer is transmitted even as the state evolves and is refined. Fourth, although cortical vision is hierarchically organized, many skip-layer connections exist (Figure 1), allowing for multiple paths through which information flows. Taken together, these properties have a fundamental consequence for network dynamics: the architecture produces a speed-accuracy trade off in which the initial output occurs rapidly but can be inaccurate, and the output improves gradually over time. Following McClelland (1979), we refer to such an architecture as *cascaded*. Cascaded dynamics contrast sharply with the dynamics of standard feedforward nets, which operate in sequential stages and each layer completes its computation before subsequent layers begin processing.

In this article, we construct cascaded networks by introducing propagation time delays in deep feedforward nets and treat the net as massively parallel such that the states of all units across all layers are updated simultaneously and iteratively. We focus on the ResNet architecture (He et al., 2016) and we introduce a propagation delay into each

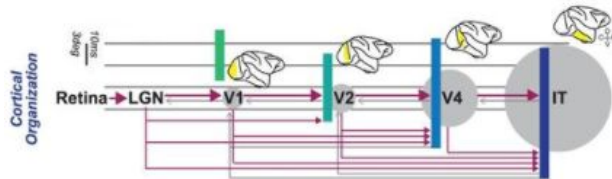


Figure 1. Simplified scheme for cortical organization of primate visual system demonstrating hierarchical and parallel systems with skip connections bypassing cortical regions. Reprinted from Cox & Maier (2015).

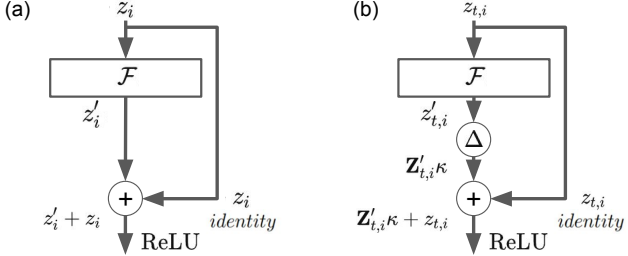


Figure 2. (a) ResNet building block; (b) Cascaded ResNet building block with a delay component (Δ) that convolves a temporal kernel with the block output. We explore delay-line and exponential-smoothing kernels.

residual block, as sketched in Figure 2. Because the skip connections—the identity mapping in the Figure—permit faster transmission of more primitive perceptual representations, the functional depth of the resulting architecture increases over time, yielding a trade off between processing speed and complexity of processing. Although we focus on the ResNet, our approach can be incorporated into any existing model that has skip connections (e.g., Highway Nets: Srivastava et al., 2015; DenseNet: Huang et al., 2017; U-Net: Ronneberger et al., 2015).

The focus of our work is on developing training procedures for cascaded architectures, understanding the temporal dynamics of cascaded architectures, and investigating their computational consequences—both costs and benefits. We propose a temporal-difference (TD; Sutton, 1988) form of the cross-entropy loss to train the cascaded architecture to obtain an accurate response as quickly as possible. We refer to this model as CASCADEDTD. We compare CASCADEDTD to two alternatives, CASCADEDSEQ and SEQUENTIAL, both of which utilize the weights of a ResNet pretrained in the standard manner. CASCADEDSEQ applies these weights to a cascaded architecture, and SEQUENTIAL uses standard layer-by-layer sequential dynamics. CASCADEDSEQ and SEQUENTIAL are asymptotically equivalent, although they have quite different temporal dynamics.

Our work makes five key contributions.

- We introduce a simple modification to transform any feed-forward architecture into a cascaded architecture and propose a supervised TD training procedure.
- Given truly parallel neural hardware, our TD procedure results in CASCADEDTD obtaining a strictly superior speed-accuracy profile to nets trained in the standard manner, run either in a sequential layer-by-layer manner (SEQUENTIAL) or cascaded manner (CASCADEDSEQ).
- CASCADEDTD tends to respond most rapidly to prototypical exemplars, according to three different notions of prototypicality. CASCADEDTD also tends to rapidly home in on the correct semantic family, whereas CASCADEDSEQ does not. These facts indicate that knowledge in the

TD-trained model is organized differently across layers than is knowledge in a model trained with the standard cross-entropy loss.

- CASCADEDTD is more robust to noise, persistent and transient, compared to CASCADEDSEQ and SEQUENTIAL.
- The time-varying output trace of the cascaded architecture provides useful signals for *meta-cognitive* processes—separately trained nets that make judgments about the cascaded architecture’s accuracy. A meta-cognitive net trained to perform out-of-distribution (OOD) discrimination performs far better when leveraging the temporal output history than when making a judgment based on the (static) output of SEQUENTIAL. And a meta-cognitive net trained to decide when to stop processing an input and initiate a response further improves the speed-accuracy trade-off of CASCADEDTD.

2. Related Work

Cortical parallelism. Primate visual cortex is organized in a hierarchical fashion but its connectivity is not strictly sequential layer-to-layer. Felleman & Van Essen (1991) identified 305 connections amongst 32 visual and visual-association areas in the primate cerebral cortex, showing a degree of connectivity between visual regions close to 40%. This massive connectivity coupled with neurophysiological principles (Gerstner et al., 1997) imbues the system with massive parallelism, which neural networks lack due to the conventional usage of discrete stage processing.

Prior research on cascaded models. McClelland (1979) characterizes human mental computation from a psychological perspective in terms of a staged architecture with the stages operating in cascade. The stages accumulate information with leaky integrators. In this view of information processing, the stages operate simultaneously, passing along partial information as it becomes available rather than completing one stage before the next stage begins operation. In recent years, the term *cascade prediction* has been used to describe the prediction of information cascades in social networks (Banerjee, 1992; Huang & Chen, 2015); we mention this unrelated work only to distinguish it from our topic. The ‘cascaded’ moniker has also been applied to work on *any-time prediction*, which assumes sequential operation of layers such that after t steps, t layers have been activated, but at each step a prediction is made from the last activated layer (Hu et al., 2019), as well as to training schemes that learn one layer of the network at a time, yielding a model trained in cascade (Marquez et al., 2018). In our terminology, this framework would be considered as SEQUENTIAL. We are aware of only two deep-learning investigations of cascaded models of the form we describe. Both are focused on sequential processing, where the model state from the previous input (e.g., video frame) can be useful for effi-

ciently processing the next. We explore a related scenario with static images that have time varying noise. Fischer et al. (2018) explore a *streaming rollout* framework that includes our cascaded model. The authors’ focus is primarily on a theoretical framework to describe the variations of recurrent network roll outs in time and to explore the levels of model parallelism they imbue. The authors very briefly explore the temporal dynamics of cascaded models showing benefits to early predictions. Carreira et al. (2018) present a causal video understanding model that performs depth-parallel computation with the objective of improving video processing efficiency via the maximizing throughput, minimizing latency, and reducing clock cycles. Both of these works perform supervised training to attain the correct model classification at each step; this training procedure is equivalent to a degenerate case of temporal difference learning, TD(1), which we show to have inferior performance. Interestingly, a variety of non-cascaded models, both recurrent (Zamir et al., 2017; Iuzzolino et al., 2019) and feedforward (Bulat & Tzimiropoulos, 2017; Newell et al., 2016), aim to reduce the number of computational steps required to obtain an accurate output. All of these models use TD(1) for training.

3. Cascaded Deep Networks

Many modern deep architectures—including ResNet (He et al., 2016), Highway Nets (Srivastava et al., 2015), DenseNet (Huang et al., 2017), U-Net (Ronneberger et al., 2015)—incorporate skip connections that bypass strictly layered feedforward connectivity, analogous to the architecture of visual cortex (Felleman & Van Essen, 1991). Under the biological assumption that signals transmitted through a neural layer are delayed relative to signals that bypass the layer, we construct a cascaded model using ResNets by introducing a novel computational component that delays the transmission of signals from the output of each computational layer, denoted Δ in Figure 2. Because these delays extend processing in time, the hidden states require a time index. The input to ResNet block i at time t is denoted $\mathbf{z}_{t,i}$. The block transforms this input via the residual transform, yielding $\mathbf{z}'_{t,i} = \mathcal{F}(\mathbf{z}_{t,i})$. We conceive of Δ as a tapped delay-line memory of the transform history, $\mathbf{Z}'_{t,i} = [\mathbf{z}'_{t,i} \ \mathbf{z}'_{t-1,i} \ \dots \ \mathbf{z}'_{1,i}]$, which is convolved with a temporal kernel κ to produce the block output

$$\mathbf{z}_{t,i+1} = \text{ReLU}(\mathbf{z}_{t,i} + \mathbf{Z}'_{t,i} \kappa). \quad (1)$$

With kernel $\kappa = [1 \ 0 \ 0 \dots 0]$, we recover the standard ResNet in which communication between layers is instantaneous. We consider two kernels to introduce time delays. With $\kappa = [0 \ 1 \ 0 \ 0 \dots 0]$, a discrete one-step delay is introduced (OSD for short). With $\kappa = (1 - \alpha)[1 \ \alpha \ \alpha^2 \ \alpha^3 \dots]$, we obtain exponentially weighted smoothing (EWS for short), with larger $\alpha \in [0, 1)$ producing slower transmission

times. Note that both of these special kernels have efficient implementations. The OSD kernel can be implemented with a one-element queue. The EWS kernel can be implemented by an incremental update and a finite (one-step) state vector:

$$\mathbf{Z}'_{t,i} \kappa = \alpha \mathbf{Z}'_{t-1,i} \kappa + (1 - \alpha) \mathbf{z}'_{t,i}.$$

We use the OSD kernel for training all models. All experiments use a ResNet-18, which has 9 residual blocks and hence 9 time delays. We also add a time delay to the output of the model’s first convolutional layer. Consequently, with the OSD kernel, the cascaded model requires 10 updates for the output to reach asymptote. At asymptote, the cascaded model is guaranteed to produce the same output as would the standard SEQUENTIAL model with the same weights.

To obtain a finer granularity of time at evaluation, some simulations switch to the EWS kernel with $\alpha = 0.9$. The model’s temporal dynamics are qualitatively similar whether OSD or EWS is used, but using EWS allows us to better distinguish individual examples in terms of their temporal dynamics. EWS with $\alpha = 0.9$ requires about 70 steps for the output to asymptote. The choice of α over a had no impact on our findings, as long as it slowed transmission.

3.1. Training Cascaded Networks with $\text{TD}(\lambda)$

Our SEQUENTIAL model is a standard ResNet, which we train as detailed in Appendix A. Our CASCADINGSEQ model uses the weights from the standard ResNet but at evaluation is run as a cascaded model. Our CASCADINGTD model is trained from scratch using the OSD kernel with the goal of producing the correct output as quickly as possible. CASCADINGTD is unrolled for T steps and trained with back propagation through time, where T is the number of delay components in the model. To encourage correct outputs sooner, we use the methods of temporal differences (TD; Sutton, 1988). Readers may associate TD methods with reinforcement learning because TD methods have traditionally been used to predict future rewards. However, TD methods are fundamentally designed for supervised learning. We use TD to predict a future outcome—the correct classification of an image—from a sequence of successively more informative states—the cascaded information flowing through the ResNet.

$\text{TD}(\lambda)$ specifies a target output y_t at each time $t \in \{1, \dots, T\}$ based on the model’s actual output \hat{y}_{t+i} at future times $t + i$ for $i > 0$, and the eventual outcome or true target, y_{true} :

$$y_t = (1 - \lambda) \left[\sum_{i=1}^{T-t} \lambda^{i-1} \hat{y}_{t+i} \right] + \lambda^{T-t} y_{\text{true}}, \quad (2)$$

where $\lambda \in [0, 1]$ is a free parameter that essentially specifies the time horizon for prediction. $\text{TD}(1)$ predicts the eventual outcome at each step; $\text{TD}(0)$ predicts the model’s

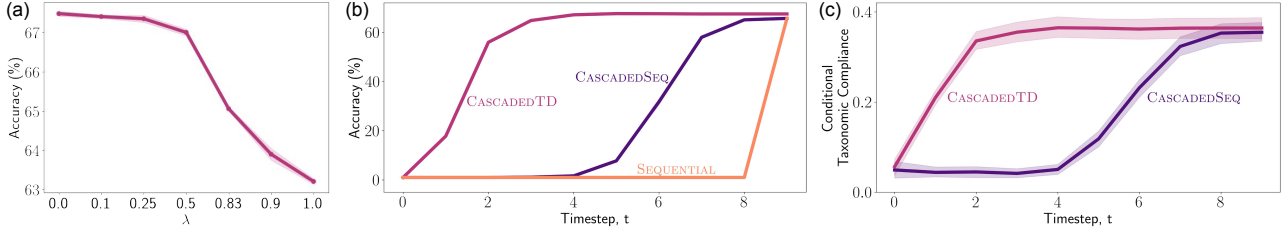


Figure 3. CIFAR-100: (a) asymptotic test accuracy as a function of λ for CASCADINGTD. (b) speed-accuracy trade off curves. (c) conditional taxonomic compliance. All graphs are based on 5 runs of each model with different random initializations. Shaded error bands—hard to see on some curves—reflect ± 1 SEM, corrected to remove performance variance unrelated to the effect of the variable on the horizontal graph axis (Masson & Loftus, 2003).

output at the next step (and the eventual outcome at the final step). Given target y_t and actual output \hat{y}_t , we specify a cross-entropy loss, $\mathcal{L} = \sum_{t=0}^T H(y_t, \hat{y}_t)$, where $H(p, q)$ is the cross-entropy. Note that y_t must be treated as a constant, not as a differentiable variable; TensorFlow and Jax require a `stop_gradient`, PyTorch instead uses `requires_grad=False`. Although Equation 2 requires knowledge of all subsequent network states, the beauty of TD methods is that this loss can be computed incrementally (Appendix A.2.1). The edge cases TD(0) and TD(1) have particularly trivial implementations. Past research has always used TD(1) for specifying intermediate targets, but we will show that TD(1) is suboptimal because the model is penalized for being unable to classify correctly at the earliest steps.

4. Results

4.1. TD(λ) Training

We conducted a sweep over hyperparameter λ to determine its effect on asymptotic accuracy of CASCADINGTD. Figure 3a shows results from five replications of CASCADINGTD on CIFAR-100. The hyperparameter has a systematic effect, consistent with classic studies with linear models (Sutton & Barto, 2018, Chapter 12). We also conducted simulations with CIFAR-10 and TinyImageNet that produce clear inverted-U curves for accuracy versus λ (Figures A.3a, A.4a). Importantly, the choice of $\lambda = 1$, which is the standard approach to training models to obtain an accurate response sooner, obtains the poorest performance for all three data sets, significantly worse than $\lambda < .5$. The essential explanation is that larger λ penalize the network for behavior it does not have the capability to achieve: obtaining the asymptotic prediction at the earliest time steps. To paraphrase the classic illustration of TD from Sutton (1988), if the task is predicting the weather on December 31, no model can predict as accurately on December 1 as on December 30. Selecting $\lambda < 1$ shortens the prediction horizon; $\lambda = 0$ corresponds with requiring a prediction only of the weather on the next day.

For CIFAR-100, CASCADINGTD’s asymptotic accuracy for

$\lambda = 0$ is 67.5% (SEM 0.1%), which is significantly better than the accuracy of 65.6% (SEM 0.1%) achieved by both SEQUENTIAL and CASCADINGSEQ, whose weights are based on the standard cross-entropy loss¹. This boost in accuracy with TD training is quite surprising considering that TD training imposes constraints on the output at each time, not just the asymptotic output. The accuracy boost suggests that TD training encourages the network to reorganize its knowledge in a manner that is beneficial for generalization, a point that we explore shortly. However, no boost is observed for CIFAR-10 (TD: 91.7%, SEM 0.2%; standard: 91.9%, SEM 0.1%) and a slight drop is observed for TinyImageNet (TD: 52.3%, SEM 0.07%; standard: 52.5%, SEM 0.06%), so it remains to be determined whether TD training might be a boon not only for cascaded models but also for models that will be run in the sequential layer-by-layer mode.

Because we focus on CIFAR-100 in the main article, and because TD(0) has a particularly trivial implementation relative to $\lambda > 0$ (there is no need for eligibility traces), we use TD(0) in all following simulations.

4.2. Speed-Accuracy Trade Offs

Under the dedicated-hardware assumption that all layers in a model can update in parallel at each time step, we can compute accuracy of response as a function of time. Figure 3b presents accuracy as a function of time on CIFAR-100. SEQUENTIAL yields no meaningful output until the final time step, as it does not exploit hardware parallelism. CASCADINGSEQ, obtained by cascading the SEQUENTIAL model at test-time, does produce a speed-accuracy trade off but it takes about four updates to begin producing meaningful output. In contrast, CASCADINGTD, trained as a cascaded model using TD(0) to encourage the network to quickly yield correct responses, shows a strictly superior speed-accuracy profile over CASCADINGSEQ. Similar results are obtained for CIFAR-10 and TinyImageNet (Figures A.3b, A.4b).

¹ Kaya et al. (2019) achieves 69.7% accuracy on CIFAR-100 with ResNet-56; we use ResNet-18 and focus on the relative performance of temporal difference training methods.

Beyond investigating the time course of fine-grain classification, we also examined coarse-grain classification. Forming twenty superclasses from the 100 fine-grain classes of CIFAR-100, as specified in Krizhevsky et al. (2009), we examined the probability of correct coarse-grain classification conditional on incorrect fine-grain classification. Zamir et al. (2017) refer to this probability as *taxonomic compliance*, which reflects information being transmitted about coarse category even when the specific class cannot be determined. As shown in Figure 3c, taxonomic compliance rises faster for CASCADINGTD than for CASCADINGSEQ. Whereas chance compliance is .05, CASCADINGTD achieves a compliance probability of .35 after 2 steps. CASCADINGSEQ requires 8 steps to achieve the same performance.

To understand the implication of Figures 3b,c for how the ResNet organizes knowledge, we need to discuss the flow of information in the cascaded model. At time 1, only the first residual block has received meaningful input, and the output is therefore based only on this block’s computation. At time 2, *all* higher residual blocks have received input from block 1, and the output is therefore based on *all* blocks’ computations, though blocks 2 and above have deficient input. At each subsequent time, all blocks are receiving meaningful input, but it is not until time t that block t has reached its asymptotic output because its input does not stabilize until $t-1$ (Figure A.1 depicts this flow of information over time). Because it takes t steps for information to *completely* propagate through t layers, one can argue that the network’s *functional depth* increases over time. That CASCADINGTD makes classification decisions above chance after 1 step indicates that the functional depth of the model has flattened relative to CASCADINGSEQ. In essence, TD training encourages the model to behave more like a WideResNet (Zagoruyko & Komodakis, 2016) than a standard deep ResNet.

4.3. Stratifying Instances by Selection Latency

Having examined the response profile of our models over an evaluation set, we now turn to analyzing the response to individual instances. Specifically, we ask about the time course of reaching a classification decision. We define the *selection latency* for an instance to be the minimum number of steps required for the classifier to reach a confidence threshold for a particular class and maintain that level going forward, i.e., $\min\{t \mid [\exists j \mid \hat{y}_{t',j} > \theta \forall t' \geq t]\}$, where \hat{y} is the model output, j is an index over classes, and θ is the threshold. The selection latency does not specify whether or not the chosen class is correct. We picked a threshold such that only $\sim 10\%$ of the test examples failed to reach threshold, $\theta = 0.83$; reported results are robust to this θ .

Having determined a selection latency for most evaluation instances, we now consider key factors that determine the latency. Our basic finding is that selection latency is inversely

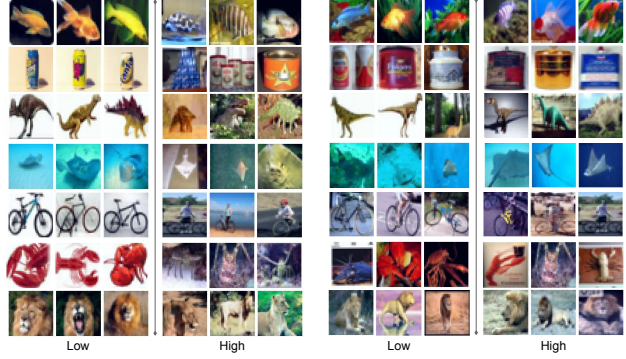


Figure 4. CIFAR-100 examples of low and high *selection latency* resulting from CASCADINGTD (left) and CASCADINGSEQ (right). related to instance prototypicality: the more prototypical instances are classified quicker.

Figure 4 shows sets of instances of various classes determined by the selection latency of the CASCADINGTD and CASCADINGSEQ models (left and right halves of the figures, respectively). In each row are instances from a particular class. The leftmost three images have the lowest selection latency (easy to classify), the rightmost three images have the highest selection latency (hard). We note the homogeneity of the low-latency images for CASCADINGTD, where most objects are against a solid background with no clutter in the image; in contrast, the high-latency images have complex backgrounds, such as the fish of varying shapes and colors. The low-latency images might be described as prototypical and the high-latency images as outliers. Turning to CASCADINGSEQ, no such pattern is evident; the instances do not appear to stratify by complexity or typicality. In the rest of this section, we formalize the notion of prototypicality and explore its relationship to selection latency. We define three measures of prototypicality; for each of these measures, a larger value means more prototypical.

- *Centrality*. We compute the cosine distance of an instance’s embedding (the penultimate layer activation) and the target-class weight vector. The larger this quantity, the better aligned the two vectors are. Because the weight vector will tend to point near the center of class instances, the cosine distance is a measure of instance centrality.
- *C-score*. Jiang et al. (2020) describe an instance-based measure of statistical regularity called the C-score. The C-score is an empirical estimate of the probability that a network will generalize correctly to an instance if it is held out from the training set. It reflects statistical regularity in that an instance similar to many other instances in the training set should have a high C-score.
- *Human labeling consistency*. Peterson et al. (2019) collected human labels on images. Most images are consistently labeled, but some are ambiguous. The negative entropy of the response distribution indicates inter-human labeling agreement. Presumably consistently labeled in-

Table 1. Spearman rank correlations between three measures of instance prototypicality and selection latency. Larger coefficient indicates faster responses for more prototypical instances.

Measure	Spearman’s ρ	
	CASCADEDSEQ	CASCADEDTD
centrality	0.140	0.352
C-score	0.326	0.489
human consistency	0.153	0.142

stances are more prototypical.

All three measures are available only for the CIFAR-10 training set. Consequently, we ran 10-fold cross validation on the training set, assessing the correlation based on the held out images in each fold. To obtain some granularity on the selection latency, we use the EWS kernel.

Table 1 presents the correlation—Spearman’s ρ —between the three prototypicality measures and negative selection latency for CASCADEDSEQ and CASCADEDTD. A positive coefficient indicates shorter latency for prototypical instances. The coefficient is reliably positive ($p < .001$) for each of the three typicality measures and both models. However, CASCADEDTD obtains reliably higher correlations on two of the three measures than CASCADEDSEQ ($p < .001$). They are not significantly different on the consistency measure ($p = .29$). Thus, by these quantitative scores, the TD training procedure leads to better stratification of instances by typicality, in line with the qualitative results presented in Figure A.2. Why does TD training distinguish instances based on prototypicality? Intuitively, a prototypical instance shares features with many other class instances. Because these features are frequent in the data set, the TD loss focuses on classifying instances with those features rapidly.

4.4. Effects of Time-Varying Inputs

In this section, we explore the effects of time-varying input (TVI) in the form of noise perturbations of a single image. Because the external environment can change more rapidly than any snapshot of the environment can be processed, the cascaded model will necessarily integrate signals from multiple snapshots. We observe a consistent benefit of CASCADEDTD over CASCADEDSEQ or SEQUENTIAL.

Figure 5 shows the six types of noise we consider on CIFAR-10 images. From left-to-right, top-to-bottom: (1) *Focus*: a 16×16 foveated patch randomly placed within the image, where regions outside of the patch are Gaussian blurred; (2) *Perlin*: gradient noise randomly applied to 40% of the image; (3) *Translation*: random shifts ± 8 pixels in (x, y) on a reflection-padded image; (4) *Occlusion*: a 16×16 occluding patch randomly placed within the image; (5) *Resolution*: random downsampling by factors of $0 \times$, $2 \times$, or $4 \times$ via average pooling followed by k -nearest upsampling to recover the original dimensionality of 32×32 . (6) *Rotation*:



Figure 5. Noise types. Top row from left to right: *Focus*, *Perlin*, *Translation*; Bottom row: *Occlusion*, *Resolution*, *Rotation*.

random rotations $\pm 60^\circ$ on a reflection padded image. Four of the perturbations are lossy; only rotation and translation are roughly information preserving.

For each noise type, a SEQUENTIAL and a CASCADEDTD model are trained with the corresponding image transformation type as a data augmentation. (CASCADEDSEQ inherits weights from SEQUENTIAL.) The training details of Appendix A are followed, except that we discard the 8×8 block data augmentation in order to avoid biasing the models toward the *Occlusion* noise transformation. We evaluate the cascaded models with the OSD kernel to allow for a comparison of cascaded models with SEQUENTIAL.

In a first experiment, TVI.1, the six noise types are persistent: the same noise source transforms the image on each time step over the entire time course of processing. We assess asymptotic (final step) accuracy on evaluation-set examples. In this setting, we treat the SEQUENTIAL model as being capable of computing a complete input-to-output activation pass at every time step, as opposed to assuming that we are operating on truly parallel hardware, which provides the cascaded models a 10-fold advantage.

Given the stateful nature of the CASCADEDTD model, we hypothesize that it will outperform SEQUENTIAL and CASCADEDSEQ for lossy noise types due to being capable of integrating information over time. The results in Table 2 support our hypothesis; the asymptotic test-set accuracy of the CASCADEDTD model is significantly higher than that of the SEQUENTIAL and CASCADEDSEQ models for the four lossy noise transformations, suggesting that training with TD encourages the cascaded model to integrate information over time allowing for more robust representations lead to improved accuracy under lossy, time-varying inputs.

Table 2. TVI.1 experiment on persistent noise. Highlight indicates best asymptotic performance for a given noise type.

TVI.1	Asymptotic Model Performance			
	Noise	SEQUENTIAL	CASCADEDSEQ	CASCADEDTD
Focus	84.27 ± 0.06	83.75 ± 0.10	87.31 ± 0.04	
Occlusion	86.26 ± 0.08	82.73 ± 0.09	89.76 ± 0.05	
Perlin	85.18 ± 0.03	84.56 ± 0.05	87.67 ± 0.08	
Resolution	84.53 ± 0.07	85.40 ± 0.07	88.19 ± 0.10	
Rotation	89.11 ± 0.04	73.79 ± 0.10	87.51 ± 0.03	
Translation	87.55 ± 0.12	76.72 ± 0.09	83.42 ± 0.14	



Figure 6. TVI.2 experiment setup. From top to bottom: *Occlusion*, *Focus*, *Resolution*, *Perlin*, *Rotation*, *Translation*.

Conversely, *SEQUENTIAL* is best on information preserving transformations such as *Translation* and *Rotation* because it is performing a full inference pass on the input whereas the cascaded models are performing a single update step.

In a second experiment, TVI.2, we present the noise-free input for 10 time steps (sufficient for the cascaded models to reach asymptote), apply one of the six noise transforms for N time steps, and then present the noise-free input for another 10 steps, allowing the model to return to its asymptotic state (Figure 6). We run five trials per condition for each $N \in \{1, 2, 3, 4, 5, 6\}$. Performance is evaluated as the drop-in-integrated-performance, $DIP = \hat{y}_T - \mathbb{E}_{t \in \{B, \dots, T\}}[\hat{y}_t]$, where T is the total time steps in the simulation, B is the onset time of the noise transformations, and \hat{y}_t is the model’s target-class confidence at time step t . DIP indicates how quickly a model can recover from noise perturbations.

On the whole, *CASCADEDTD* is more robust to transient perturbations than *SEQUENTIAL* and *CASCADEDSEQ* (Table 3). *SEQUENTIAL* has a disadvantage in being unable to perform noise cancellation by combining signals across frames, yet it has a massive advantage in performing ten sequential updates per time step, versus one parallel update for the cascaded models. While both *CASCADEDTD* and *CASCADEDSEQ* smooth responses over frames, *CASCADEDTD* performs better, indicating that beyond smoothing, TD training orchestrates the integration of image-specific perceptual information. This integration matters more for lossy transformations, where information integration is essential.

4.5. Meta-cognitive Inference

In this section, we consider the hypothesis that temporally intermediate outputs from cascaded networks can provide additional signals to improve performance. We term this *metacognition*, by reference to human abilities to reason about our reasoning processes. For example, we might want to greet an acquaintance by name, but if their name comes to mind only after a long lag, we might lack the confidence to speak their name out loud and instead choose a less personal

Table 3. TVI.2 experiment on transient noise. Highlight indicates lowest DIP for a given noise type.

TVI.2	Drop in Integrated Performance (DIP)			
	NOISE	SEQUENTIAL	CASCADEDSEQ	CASCADEDTD
Focus	0.62 ± 0.04	0.66 ± 0.05	0.00 ± 0.01	
Occlusion	7.70 ± 0.55	8.25 ± 0.72	0.93 ± 0.15	
Perlin	0.86 ± 0.06	0.87 ± 0.07	0.00 ± 0.01	
Resolution	0.81 ± 0.06	0.53 ± 0.05	0.18 ± 0.02	
Rotation	0.24 ± 0.02	4.12 ± 0.29	0.00 ± 0.01	
Translation	0.72 ± 0.05	4.17 ± 0.37	1.53 ± 0.14	

greeting. To map this scenario to our present setting, we explore the idea of using the temporal trace of output from the cascaded model to train a separate classifier, which we call *METACOG*, to make judgments about the performance of the cascaded model. The particular judgments are OOD detection and deciding when to commit to a response.

4.5.1. OUT-OF-DISTRIBUTION DETECTION

In this set of experiments, we utilize the output of *CASCADEDTD* to train *METACOG* *discriminatively* for OOD detection and show that it significantly outperforms models trained using only the asymptotic *CASCADEDTD* output. *METACOG* is a multi-layer perceptron with a 256-unit hidden layer and a sigmoidal output unit for binary prediciton: 1 or 0 for in- or out-of-distribution instances, respectively. CIFAR-10’s validation set serves as the in-distribution training examples, whereas the validation sets of TinyImageNet, LSUN, and SVHN serve as OOD training examples, with crop and resize variations to TinyImageNet and LSUN following Liang et al. (2017); see details in Appendix B.1. One *METACOG* model is trained per (in-, out-of-distribution) dataset pairing—e.g., (CIFAR-10, SVHN)—and input representation type (discussed below). The respective test set is used for evaluation. The *CASCADEDTD* output serves as input to *METACOG* and is represented in one of four ways: (1) the confidence of the most probable class, known as the *max softmax prediction* or *MSP*, (2) entropy of the class posterior distribution, (3) the class posterior distribution, or (4) the logit representation of the posterior. We investigate whether feeding the output of all time steps to *METACOG* leads to improved prediction relative to feeding only the final asymptotic output. In a standard feedforward net, only the latter information is available.

A baseline metric is computed directly from the max softmax predictions of the *CASCADEDTD* model, whereas the meta-cognitive metrics are computed by averaging accuracy over dataset pairings. Following Liang et al. (2017), we assess OOD performance with *AUROC*, the Area Under the Receiver Operating Characteristic curve, and *FPR* @ 95% *TPR*, the false positive rate at 95% true positive rate.

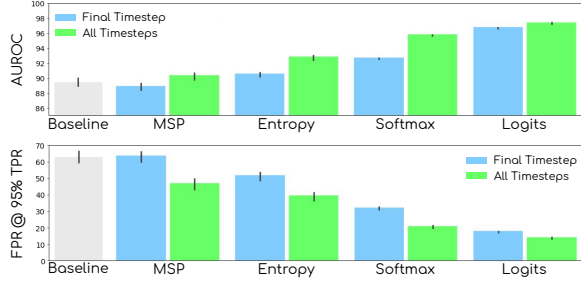


Figure 7. CASCADINGTD+METACOG results for OOD detection. Error bars reflect ± 1 SEM corrected to remove random variance (Masson & Loftus, 2003). Leveraging temporal information (All Time steps) yields significantly improved performance for all representations, with All Time step Logits affording the best overall performance.

Using the temporal dynamics significantly improves OOD detection performance on both metrics regardless of representation used (Figure 7). Additionally, the logit representation obtains the best performance of all the representations considered (see Table B.3 for quantitative results).

4.5.2. RESPONSE INITIATION

Lastly, we explore the use of METACOG for deciding when to initiate a response. That is, given the output sequence from CASCADINGTD up to time t , should the most probable class label at t be chosen, or should processing continue at least through $t + 1$? We train a METACOG model and show significant improvements in the model’s speed-accuracy trade off. Because we need to provide a varying-length input history to METACOG, we use a GRU recurrent net (Cho et al., 2014). The GRU ingests the sequence of logits and produces a scalar output. METACOG is trained with a cross-entropy loss summed over time steps to output 1 if CASCADINGTD’s current class-label prediction matches its asymptotic prediction, otherwise 0. See Appendix B.3 for additional training details.

For evaluation, we test when METACOG reaches a given threshold, θ , and determine model mean accuracy and stopping time for that θ . Varying θ , we obtain a speed-accuracy curve which can be compared to CASCADINGTD’s original curve (Figure 8). The outcome is a significant decrease in latency for a given level of accuracy, e.g., the latency is approximately cut in half for an accuracy of 85%. The same analysis was conducted with CASCADINGSEQ, and we found a similar but smaller speed up (Figure A.5). Nonetheless, CASCADINGTD remained more efficient than CASCADINGSEQ.

5. Discussion

Our exploration of the temporal dynamics of cascaded deep networks has addressed a range of topics, including: speed-accuracy trade offs, understanding what makes images ‘easy’

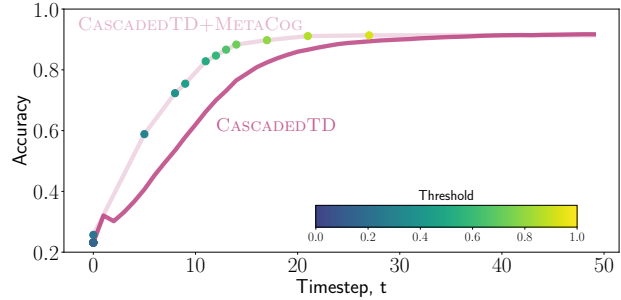


Figure 8. Comparing the speed-accuracy curve for CASCADINGTD vs. CASCADINGTD+METACOG.

(classified quickly) and ‘hard’ (classified slowly), moderating time-varying input noise, and demonstrating that the temporal trace of a network’s output provides an additional signal that can be exploited to improve information processing. We hope to have convinced readers that cascaded models have interesting properties and are a promising avenue of exploration. We see three directions in which cascaded nets have particular potential.

- For neuroscientists using deep nets as a model of human vision, cascaded nets are a better approximation to the dynamics of the neural hardware. The properties we investigate—neurons operate in parallel, neurons are stateful, and neurons are slow to transmit information—seem likely to have a critical impact on the nature of cortical computing. As one simple illustration, cortical feedback processes are often posited to be critical for explaining difference in processing efficiency of visual stimuli (e.g., Kar et al., 2019; Spoerer et al., 2017), but we have shown that these difference might well be explained by feedforward cascaded dynamics.
- For hardware researchers, cascaded networks are a possible direction for the future design of AI hardware. It is a direction quite unlike modern GPUs and TPUs, one that exploits massively parallel albeit slow and possibly noisy information processing. Our success in showing strong performance from cascaded models, as well as a training procedure to obtain quick and accurate responses, should encourage researchers in this hardware direction.
- For AI researchers, even those who care nothing about cascaded models per se, cascaded models offer two innovations. First, they offer a promising and unusual way to train feedforward models. One can take a feedforward model, turn it into a cascaded model for training with TD methods, and then run it in SEQUENTIAL mode. SEQUENTIAL mode will obtain the same outcome as the asymptotic output of a cascaded model. We’ve shown that TD training can improve asymptotic model accuracy due to inductive biases it imposes on the organization of representations. Further investigations will be needed to understand the conditions under which this improvement

occurs. Second, our explorations of metacognition are, to the best of our knowledge, a new direction for the field, perhaps because the temporal dimension is critical to obtaining a representation that is rich enough that it can be mined for insight into the operation of a network.

References

- Banerjee, A. V. A simple model of herd behavior. *The quarterly journal of economics*, 107(3):797–817, 1992.
- Bulat, A. and Tzimiropoulos, G. How far are we from solving the 2D & 3D face alignment problem? In *Proceedings of the IEEE International Conference on Computer Vision*, pp. 1021–1030, 2017.
- Carreira, J., Patraucean, V., Mazare, L., Zisserman, A., and Osindero, S. Massively parallel video networks. In *Proceedings of the European Conference on Computer Vision (ECCV)*, pp. 649–666, 2018.
- Cho, K., Van Merriënboer, B., Bahdanau, D., and Bengio, Y. On the properties of neural machine translation: Encoder-decoder approaches. *arXiv preprint arXiv:1409.1259*, 2014.
- Cox, M. A. and Maier, A. Serial versus parallel processing in mid-level vision: filling-in the details of spatial interpolation. *Neuroscience of consciousness*, 2015(1), 2015.
- Deng, J., Dong, W., Socher, R., Li, L.-J., Li, K., and Fei-Fei, L. Imagenet: A large-scale hierarchical image database. In *2009 IEEE conference on computer vision and pattern recognition*, pp. 248–255. Ieee, 2009.
- Felleman, D. J. and Van Essen, D. C. Distributed hierarchical processing in the primate cerebral cortex. In *Cereb cortex*. Citeseer, 1991.
- Fischer, V., Köhler, J., and Pfeil, T. The streaming rollout of deep networks-towards fully model-parallel execution. In *Advances in Neural Information Processing Systems*, pp. 4039–4050, 2018.
- Fukushima, K. Neocognitron: A self-organizing neural network model for a mechanism of pattern recognition unaffected by shift in position. *Biological Cybernetics*, 36:193–202, 1980.
- Gerstner, W., Kreiter, A. K., Markram, H., and Herz, A. V. Neural codes: firing rates and beyond. *Proceedings of the National Academy of Sciences*, 94(24):12740–12741, 1997.
- He, K., Zhang, X., Ren, S., and Sun, J. Deep residual learning for image recognition. In *Proceedings of the IEEE conference on computer vision and pattern recognition*, pp. 770–778, 2016.
- Hu, H., Dey, D., Hebert, M., and Bagnell, J. A. Learning anytime predictions in neural networks via adaptive loss balancing. In *Proceedings of the AAAI Conference on Artificial Intelligence*, volume 33(01), pp. 3812–3821, 2019.
- Huang, G., Liu, Z., Van Der Maaten, L., and Weinberger, K. Q. Densely connected convolutional networks. In *Proceedings of the IEEE conference on computer vision and pattern recognition*, pp. 4700–4708, 2017.
- Huang, S.-L. and Chen, K.-C. Information cascades in social networks via dynamic system analyses. In *2015 IEEE international conference on communications (ICC)*, pp. 1262–1267. IEEE, 2015.
- Iuzzolino, M., Singer, Y., and Mozer, M. C. Convolutional bipartite attractor networks. *arXiv preprint arXiv:1906.03504*, 2019.
- Jiang, Z., Zhang, C., Talwar, K., and Mozer, M. C. Characterizing structural regularities of labeled data in over-parameterized models. *arXiv e-prints*, art. *arXiv preprint arXiv:2002.03206*, 2020.
- Kar, K., Kubilius, J., Schmidt, K., Issa, E. B., and DiCarlo, J. J. Evidence that recurrent circuits are critical to the ventral stream’s execution of core object recognition behavior. *Nature Neuroscience*, 04/2019 2019.
- Kaya, Y., Hong, S., and Dumitras, T. Shallow-deep networks: Understanding and mitigating network overthinking. In *International Conference on Machine Learning*, pp. 3301–3310. PMLR, 2019.
- Kriegeskorte, N. Deep neural networks: A new framework for modeling biological vision and brain information processing. *Annual Review of Vision Science*, 1(1):417–446, 2015.
- Krizhevsky, A., Hinton, G., et al. Learning multiple layers of features from tiny images. 2009.
- Liang, S., Li, Y., and Srikant, R. Enhancing the reliability of out-of-distribution image detection in neural networks. *arXiv preprint arXiv:1706.02690*, 2017.
- Lindsay, G. W. Convolutional neural networks as a model of the visual system: Past, present, and future. *Journal of Cognitive Neuroscience*, 0(0):1–15, 2020. doi: 10.1162/jocn_a_01544. URL https://doi.org/10.1162/jocn_a_01544. PMID: 32027584.
- Marquez, E. S., Hare, J. S., and Niranjan, M. Deep cascade learning. *IEEE transactions on neural networks and learning systems*, 29(11):5475–5485, 2018.

- Masson, M. E. and Loftus, G. R. Using confidence intervals for graphically based data interpretation. *Canadian Journal of Experimental Psychology/Revue canadienne de psychologie expérimentale*, 57(3):203, 2003.
- McClelland, J. L. On the time relations of mental processes: an examination of systems of processes in cascade. *Psychological review*, 86(4):287, 1979.
- Netzer, Y., Wang, T., Coates, A., Bissacco, A., Wu, B., and Ng, A. Y. Reading digits in natural images with unsupervised feature learning. 2011.
- Newell, A., Yang, K., and Deng, J. Stacked hourglass networks for human pose estimation. In *European conference on computer vision*, pp. 483–499. Springer, 2016.
- Peterson, J. C., Battleday, R. M., Griffiths, T. L., and Russakovsky, O. Human uncertainty makes classification more robust. In *Proceedings of the IEEE International Conference on Computer Vision*, pp. 9617–9626, 2019.
- Ronneberger, O., Fischer, P., and Brox, T. U-net: Convolutional networks for biomedical image segmentation. In *International Conference on Medical image computing and computer-assisted intervention*, pp. 234–241. Springer, 2015.
- Spoerer, C. J., McClure, P., and Kriegeskorte, N. Recurrent convolutional neural networks: A better model of biological object recognition. *Frontiers in Psychology*, 8:1551, 2017. URL <https://www.frontiersin.org/article/10.3389/fpsyg.2017.01551>.
- Srivastava, R. K., Greff, K., and Schmidhuber, J. Highway networks. *arXiv preprint arXiv:1505.00387*, 2015.
- Sutton, R. S. Learning to predict by the methods of temporal differences. *Machine learning*, 3(1):9–44, 1988.
- Sutton, R. S. and Barto, A. G. *Reinforcement learning: An introduction*. MIT press, 2018.
- Yu, F., Seff, A., Zhang, Y., Song, S., Funkhouser, T., and Xiao, J. Lsun: Construction of a large-scale image dataset using deep learning with humans in the loop. *arXiv preprint arXiv:1506.03365*, 2015.
- Zagoruyko, S. and Komodakis, N. Wide residual networks. *arXiv preprint arXiv:1605.07146*, 2016.
- Zamir, A. R., Wu, T.-L., Sun, L., Shen, W. B., Shi, B. E., Malik, J., and Savarese, S. Feedback networks. In *Proceedings of the IEEE Conference on Computer Vision and Pattern Recognition*, pp. 1308–1317, 2017.

A. Experiment Details

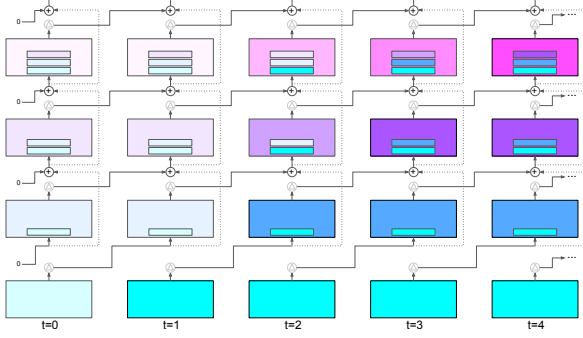


Figure A.1. A cascaded network, unrolled over time. Each column represents a four block ResNet. The blocks (rectangles) may consist of two or more convolutional layers, with a one-step delay (OSD) kernel at the output of each block, indicated by the Δ node. The OSD kernel has the effect of causing the output of block i at step t to feed into the input to block $i+1$ at step $t+1$, as indicated by the solid lines. Due to the skip connections, the output of block i at step t also propagates immediately to all higher layer blocks, as indicated by the dashed lines. The saturation (color intensity) of a block indicates the extent to which that block has reached quiescence (i.e., its activation is no longer changing because all lower blocks reached quiescence at the previous step). The small rectangles within a block signify the activation state of all blocks below that are contributing to the state of the block.

A.1. SEQUENTIAL and CASCADINGTD Experiment Details

For all SEQUENTIAL and CASCADINGTD models, we used a ResNet-18 for CIFAR-10, CIFAR-100, and TinyImageNet datasets. The models were trained using data parallelism over 8 GPUs (see §A.4 for infrastructure details), with the model on each GPU using a batch size of 128. SGD with Nesterov momentum, an initial learning rate of 0.1, weight decay of 0.005, and momentum of 0.9 was used to optimize a softmax cross-entropy loss for SEQUENTIAL and a temporal difference cross-entropy loss for CASCADINGTD. All models were trained for 200 epochs and the learning rate was decayed with a multiplicative factor of 0.2 every 30 epochs.

The training datasets were split (class-balanced) as 90-10 train-validation, where the validation splits were held out for downstream tasks, such as training METACOG models (see §4.5). For CASCADINGTD, the batch normalization layer must be augmented such that running means and variances are tracked independently for each timestep. At run-time, if the maximum number of timesteps used during training is exceeded, as occurs with the EWS kernel, the final timestep statistics of the batch normalization layers are used for all subsequent timesteps. Furthermore, we observed that the offset parameter of the affine transformation of the batch normalization on identity mappings explode during training; consequently, we do not use batch normalization on the

identity mapping.

A.2. Temporal Difference Loss

A.2.1. INCREMENTAL TD FORMULATION

TD(λ) amounts to training at each time step t with a target, y_t^λ , that is an exponentially decaying trace of future outputs, anchored beyond some asymptotic time T to the true target, y . Denoting the network output at step $t \in \{1, \dots, T\}$ as \hat{y}_t , the trace is:

$$y_t^\lambda = (1 - \lambda) \sum_{n=1}^{\infty} \lambda^{n-1} \bar{y}_{t+n}$$

$$\text{with } \bar{y}_{t+n} = \begin{cases} \hat{y}_{t+n} & \text{if } t+n \leq T \\ y & \text{otherwise} \end{cases}$$

$$= (1 - \lambda) \sum_{n=1}^{T-t} \lambda^{n-1} \hat{y}_{t+n} + \lambda^{T-t} y.$$

We train with cross entropy loss over all time steps. For a single example, the loss is

$$\mathcal{L} = - \sum_{t,i} y_{ti}^\lambda \ln \bar{y}_{ti}.$$

The derivative of this loss with respect to the network parameters w can be expressed in terms of the derivative with respect to the logits:

$$\nabla_w \mathcal{L} = - \sum_{t,i} (y_{ti}^\lambda - \bar{y}_{ti}) \nabla_w z_{ti},$$

where z_{ti} is the logit of class i at step t . The temporal difference method provides a means of computing this gradient incrementally, such that at each step t , an update can be computed based on only the difference of model outputs at t and $t+1$:

$$\nabla_w^{\text{TD}} \mathcal{L} = - \sum_{t,i} (\bar{y}_{t+1,i} - \bar{y}_{ti}) e_{ti},$$

where e_{ti} is an *eligibility trace*, defined as:

$$e_{ti} = \begin{cases} 0 & \text{if } t = 0 \\ \lambda e_{t-1,i} + \nabla_w z_{ti} & \text{if } t \geq 1 \end{cases}$$

The incremental formulation of TD via $\nabla_w^{\text{TD}} \mathcal{L}$ is valuable when gradients and/or weight updates must be computed on line rather than presenting an entire sequence before computing the loss, e.g., in the situation where the network runs for many steps and truncated BPTT is required. In our experiments, we use the summed gradient, $\nabla_w \mathcal{L}$, computed by PyTorch from the full T step sequence and our exponentially weighted target, y_t^λ .



Figure A.2. CIFAR-10 examples of low and high selection latency resulting from CASCADINGTD (left) and CASCADINGSEQ (right).

A.2.2. TD(λ) SWEEP

Figures A.3a and A.4a show the asymptotic accuracy versus $\text{TD}(\lambda)$ for CIFAR-10 (5 trials per λ) and TinyImageNet (3 trials per λ), respectively. Table A.2 shows the full tabulated results for CIFAR-10, CIFAR-100, and TinyImageNet. Note, 5 trials per λ were trained for CIFAR-100.

A.3. Data Augmentation

When training SEQUENTIAL and CASCADINGTD models on CIFAR-10 and CIFAR-100, for each batch the 32×32 images are padded with 4 pixels to each border (via reflection padding), resulting in a 40×40 image. A random 32×32 crop is taken, the image is randomly flipped horizontally, and standard normalized using the training set statistics is applied. Finally, a random 8×8 block cut is taken such that the cropped pixels are set to 0. Images at run-time are only standard normalized using training set statistics - no other augmentation is applied with the exception of the persistent and transient noise experiments (see §4.4). The same process is followed for TinyImageNet with the following exceptions: (1) the 64×64 images are padded to 86×86 with reflection padding, random cropped back to 64×64 , randomly flipped horizontally, then standard normalized, and (2) no 8×8 block cutting is applied.

A.4. Computing Infrastructure

We used 8x NVIDIA Tesla V100's on Google Cloud Platform (GCP) for training all SEQUENTIAL and CASCADINGTD models; a single V100 was used for all evaluations, and to train METACOG models. All models were implemented in PyTorch v1.5.0, using Python 3.7.7 operating on Ubuntu 18.04.

A.5. Average Runtime and Reproducibility

Table A.1 shows average runtimes (in hours) and \pm SEM for training SEQUENTIAL and CASCADINGTD models on each dataset. Reproducibility was ensured in the data pipeline and model training by seeding Random, Numpy, and PyTorch packages, as well as flagging deterministic cudnn via PyTorch API. When sweeping over λ for

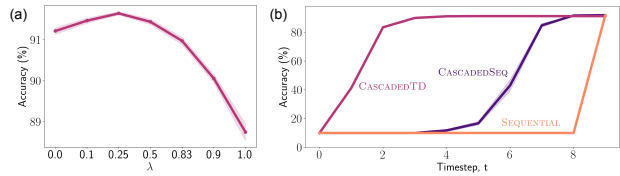


Figure A.3. CIFAR-10: (a): asymptotic test accuracy vs. λ . (b): speed-accuracy trade-off. Error bands show corrected SEM (n=5).

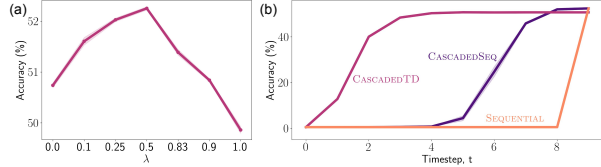


Figure A.4. TinyImageNet: (a): asymptotic test accuracy vs. λ . (b): speed-accuracy trade-off. Error bands show corrected SEM (n=5).

a given model and dataset, 5 trials, [1, 2, 3, 4, 5], were trained to obtain statistical measures; the trials map to seeds [42, 542, 1042, 1542, 2042]. All models of same architecture used identical weights upon initialization. The average runtime for training METACOG models on a single V100 GPU requires less than 3 minutes. When training multiple trials for a given METACOG model, all models are initialized with the same weights, and 42 was used to seed all packages as detailed above.

A.6. Additional Temporal Dynamics Results

We show low and high *selection latency* instances between CASCADINGTD and CASCADINGSEQ models in Figure A.2 for CIFAR-10. As with CIFAR-100, the qualitative differences between low and high *selection latency* for CASCADINGTD are stark, with low *selection latency* instances being more representative of prototypical instances of the given class (e.g., boats on blue water; horses in fields), whereas high *selection latency* instances are less typical (e.g., boats on green grass; horses in snow). Furthermore, we do not observe the strong delineation between low and high *selection latency* groups for CASCADINGSEQ, supporting the claim that TD training allows the model to more rapidly respond to *prototypical* exemplars.

Table A.1. Average runtime for training SEQUENTIAL and CASCADINGTD over CIFAR-10, CIFAR-100, and TinyImageNet.

Dataset	Model	Average Runtime (hours)
CIFAR-10	SEQUENTIAL	1.48 ± 0.002
	CASCADINGTD	1.81 ± 0.001
CIFAR-100	SEQUENTIAL	1.48 ± 0.001
	CASCADINGTD	1.83 ± 0.001
TinyImageNet	SEQUENTIAL	1.45 ± 0.035
	CASCADINGTD	1.97 ± 0.020

Table A.2. TD(λ) experiments. Green font indicates best performance across TD(λ) and SEQUENTIAL models for a given dataset. Highlight indicates best performing TD(λ) across λ 's for a given dataset.

Dataset	Model							
	TD(0)	TD(0.1)	TD(0.25)	TD(0.5)	TD(0.83)	TD(0.9)	TD(1)	SEQUENTIAL
CIFAR-10	91.22 \pm 0.18	91.48 \pm 0.14	91.65 \pm 0.08	91.45 \pm 0.16	90.98 \pm 0.21	90.07 \pm 0.24	88.75 \pm 0.42	91.91 \pm 0.08
CIFAR-100	67.48 \pm 0.14	67.41 \pm 0.09	67.35 \pm 0.20	67.00 \pm 0.18	65.06 \pm 0.11	63.90 \pm 0.33	63.20 \pm 0.14	65.56 \pm 0.06
TinyImageNet	50.74 \pm 0.11	51.60 \pm 0.17	52.03 \pm 0.07	52.25 \pm 0.07	51.39 \pm 0.13	50.84 \pm 0.07	49.86 \pm 0.15	52.46 \pm 0.06

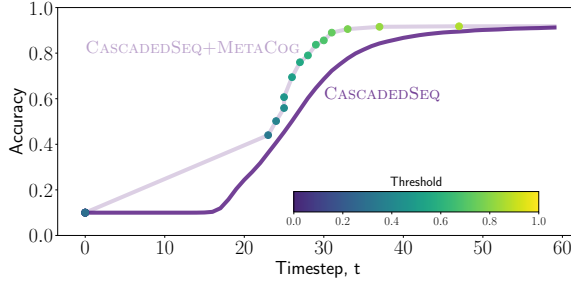


Figure A.5. Response initiation results comparing CASCADINGSEQ+META COG GRU against CASCADINGSEQ.

B. Meta-cognitive Experiment Details

For all meta-cognitive experiments, training data is generated from the EWS kernel applied to CASCADINGTD(0).

B.1. OOD Detection Dataset Details

CIFAR-10 serves as the in-distribution dataset, which contains 5,000 validation and 10,000 test set instances. The 5,000 validation instances, which we use as the in-distribution training set for OOD, were derived from a 90-10 train-validation split of the original 50,000 training instances used for training the CASCADINGTD model. The OOD datasets are as follows:

TinyImagenet The Tiny ImageNet (TinyImageNet) is a 200-class subset of ImageNet (Deng et al., 2009) and it contains 10,000 validation and 10,000 test instances. Following the methods of Liang et al. (2017) we introduce two variations: 1) *resize*; the image is downsampled to 32×32 , and 2) *crop*; a random 32×32 crop is taken from the image.

LSUN The Large-scale Scene UNderstanding (LSUN) (Yu et al., 2015) consists of 10 scenes categories, such as classroom, restaurant, bedroom, etc. It contains 10,000 validation and 10,000 test instances, and similar to TinyImageNet, we use the *resize* and *crop* variations.

SVHN The Street View House Numbers (SVHN) (Netzer et al., 2011) dataset is obtained from house numbers in Google Street View images. It consists of 73,257 validation and 26,032 test set images.

Table B.3. CIFAR-10 (in-distribution) vs. Aggregate OOD dataset quantitative measures corresponding to Figure 7. Each representation may include all time step outputs, t_{all} , or only the final output, t_{final} .

OOD Representation	AUROC	FPR @ 95% TPR
CASCADINGTD [MSP]	89.5 \pm 0.5	63.0 \pm 3.5
METACOG t_{final} [MSP]	88.8 \pm 0.5	63.0 \pm 3.1
METACOG t_{all} [MSP]	90.2 \pm 0.5	46.4 \pm 3.1
METACOG t_{final} [Entropy]	90.5 \pm 0.3	51.2 \pm 2.5
METACOG t_{all} [Entropy]	92.7 \pm 0.3	38.9 \pm 2.5
METACOG t_{final} [Softmax]	92.6 \pm 0.1	31.7 \pm 0.7
METACOG t_{all} [Softmax]	95.7 \pm 0.1	20.5 \pm 0.7
METACOG t_{final} [Logits]	96.7 \pm 0.1	17.5 \pm 0.4
METACOG t_{all} [Logits]	97.3 \pm 0.1	13.7 \pm 0.4

B.2. OOD Detection Training Details

The METACOG model is trained for 300 epochs with batch sizes of 256. We used Adam with an initial learning rate of 0.001 and weight decay of 0.0005 to optimize a binary cross entropy loss. Dropout with keep probability 0.5 was used for regularization. Numerical values corresponding to Figure 7 are tabulated in Table B.3 with reported SEM corrected to remove random variance (Masson & Loftus, 2003).

B.3. Response Initiation

The METACOG GRU is trained for 300 epochs with a batch size of 256. We used Adam with an initial learning rate of 0.0001 and weight decay of 0.0001 to optimize a binary cross entropy loss.

The METACOG model is trained on the 4,500 instances of the CIFAR-10 validation set that have been processed by the CASCADINGTD model, yielding a training set of dimension $4,500 \times 70 \times 10$, where there are 70 timesteps and 10 logit values. We generate our evaluation set from the same method above using the CASCADINGTD model on the 10,000 instance test set.

Figure A.5 shows the response initiation results comparing CASCADINGSEQ+META COG GRU with CASCADINGSEQ. Similar to the results for CASCADINGTD+META COG GRU versus CASCADINGTD, the METACOG approaches yields significant improvements to response initiation.